A&A 489, 773–776 (2008)
DOI: 10.1051/0004-6361:200809607

Astronomy & Astrophysics

On the origin of the Balmer and Lyman emission lines in solar prominences *(Research Note)*

G. Stellmacher[1] and E. Wiehr[2]

[1] Institut d'Astrophysique (IAP), 98bis Bvd. d'Arago, 75014 Paris, France
e-mail: stell@iap.fr
[2] Institut für Astrophysik, Universität Göttingen Friedrich-Hund-Platz 1, 37077 Göttingen, Germany
e-mail: ewiehr@astro.physik.uni-goettingen.de

Received 19 February 2008 / Accepted 9 July 2008

ABSTRACT

Aims. We show how the observed hydrogen Balmer and Lyman emission lines constrain the modeling of quiescent solar prominences.
Methods. We compare space observations of Lyman lines with ground-based observations of Balmer lines for quiescent solar prominences of comparable brightness defined by their Hβ emission.
Results. The effective number densities of hydrogen atoms emitting from the same upper level u deduced from the corresponding emerging Lyman and Balmer line emissions show large differences that diminish with increasing level number and converge at the highest level numbers. Hydrogen atoms excited in $u = 5$ contribute 250 times less, and those in $u = 8$ still contribute 65 times less to the Lyman than to the corresponding Balmer emission, supporting the idea of distinct spatial origin of the emissions of both series. This is also indicated by the line widths. The high optical thickness of all Lyman members allows the brightness temperature T_b to be estimated from the spectral radiance at line center, where T_b is found to be largely independent of the upper level number, in contrast to the (known) behavior of the Balmer lines.

Key words. Sun: prominences – radiation mechanisms: thermal

1. Introduction

The hydrogen spectrum of solar prominences is an important source of information about the physical state and the structure of these cool plasma clouds embedded in a hot environment. The emission lines of this most abundant element are distributed over a wide spectral range, reaching from the Lyman series in the EUV to the Balmer lines in the visible and further series in the infrared spectral regions. Large parts of the EUV Lyman lines have been observed with the SUMER spectrograph onboard SOHO by Stellmacher et al. (2003) and by Parenti et al. (2005a).

The complete Balmer series in the visible spectral range is much less frequently observed, since large dispersion spectrographs make simultaneous observations over the wide spectral range from Hα at 6563 Å to the highest Balmer members below 3880 Å difficult. Large parts of the Balmer series have been observed by Stellmacher (1969), Yakovkin & Zel'dina (1975), and Illing et al. (1975). But simultaneous observations of both the whole Lyman and the whole Balmer sequences do not exist to our knowledge.

However, data of both line series from different observations may be compared using the *mean values of prominences with similar brightness*. Here, the total line radiance of the (mostly optically thin) Hβ emission serves as a reasonable indicator. Such a relation between spectroscopic data in the EUV and in the visible spectral region may be found in De Boer et al. (1998) and Stellmacher et al. (2003) who simultaneously observed large parts of the Lyman lines from space and selected Balmer lines including Hβ from ground.

2. Comparison of observed Balmer and Lyman spectra

To compare observed Lyman and Balmer lines, we used the equation that relates the spectral line radiance E_{ul}, i.e. the spectral radiance $L_{ul}(\lambda)$ integrated over the respective emission line, with the number density of atoms, n_u, emitting from the upper level u (Unsöld 1955):

$$E_{ul} = \int L_{ul}^{\lambda}\,\mathrm{d}\lambda = \frac{h\cdot c}{4\pi}\cdot\frac{A_{ul}}{\lambda_{ul}}\cdot n_u\cdot D \qquad \text{yielding:} \qquad (1)$$

$$\log\frac{n_u D}{g_u} = \log E_{ul} - \log\frac{A_{ul}g_u}{\lambda_{ul}} + \log\frac{4\pi}{hc} = \log E_{ul} - C_{ul} + C \qquad (2)$$

where $C = \log(4\pi/(h\cdot c)) = 16.8$[cgs], A_{ul} are the Einstein coefficients for the spontaneous emission from upper level u to lower level l, and $g_u = 2\cdot u^2$ the statistical weight of the upper level u; $C_{ul} = \log(A_{ul}\cdot g_u/\lambda_{ul})$ is a constant for each line and given in the NBS-tables (Wiese et al. 1966). Equation (2) relates the observed spectral line radiance E_{ul}^{obs} and the effective number of emitting atoms $n_u D$. For emission from optically thin layers, $n_u D$ is the actual number of hydrogen atoms excited in the upper level u emitting along the line-of-sight. In the form $n_u\cdot D/g_u$ (in Eq. (2)), this quantity may be used in the Boltzmann formula.

The effective number of emitting hydrogen atoms obtained from Lyman and from Balmer lines observations are compared

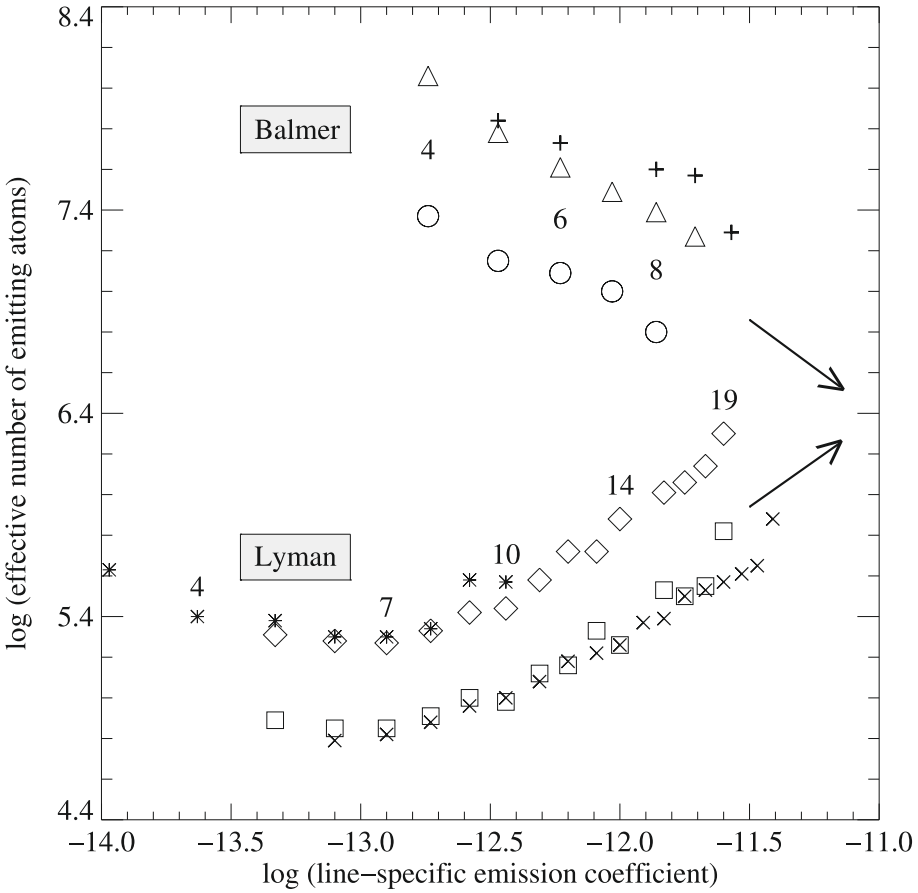

Fig. 1. Effective number of atoms, log $E_{ul}^{obs} - C_{ul} + C$, emitting from the upper level u to the lower level l, versus the line-specific emission coefficient, $C_{ul} = \log(A_{ul} \cdot g_u/\lambda_{ul})$, from observations of the Balmer series by Stellmacher (1969; circles for faint and triangles for brighter prominences) and by Illing et al. (1975; crosses) in comparison with observations of the Lyman series by Parenti et al. (2005; X), by Stellmacher et al. (2003; rhombs 42-L; squares 70-H), and by Heinzel et al. (2001; asterisks); indices give upper level numbers u.

in Fig. 1. Its upper part shows means of Balmer line observations by Stellmacher (1969) and by Illing et al. (1975), which can be considered as characteristic of moderately bright prominences with emissions $E(H\beta) \leq 2 \times 10^4$ erg/(cm^2 s sr). Substantial higher spatial resolution is achieved in the detailed photometric data of Hα and Hβ ($u = 3; 4$), obtained by Stellmacher & Wiehr (1994). The results from observations by Yakovkin & Zel'dina (1975) are not entered in Fig. 1 since they represent rare prominences with very bright emissions up to $E(H\beta) \leq 16.5 \times 10^4$ erg/(cm^2 s sr), like those discussed by Stellmacher & Wiehr (2005) and comparable Lyman observations do not exist.

For the faint and moderately bright prominences characterized by $E(H\beta) \leq 2 \times 10^4$ erg/(cm^2 s sr), EUV observations with the SUMER instrument onboard SOHO have been taken by De Boer et al. (1998) and by Stellmacher et al. (2003) simultaneously with ground-based data. These Lyman data are shown in the lower part of Fig. 1 together with EUV observations by Heinzel et al. (2001) and by Parenti et al. (2005a).

The differences in the abscissa values for equal upper level u of the Balmer and the Lyman lines arise from the different Einstein coefficients A_{ul}. The striking differences in the ordinate values $\log E_{ul} - C_{ul} + C$ of the Lyman and the Balmer lines reflect the largely different number of effectively emitting atoms. Emerging Lyman lines stem from up to 250 times less emitters than the corresponding Balmer lines from the same upper level u.

Figure 1 shows a steady decrease for the Balmer lines in the ordinate values $\log E_{ul} - C_{ul} + C$ with increasing upper level u, and this reflects the decreasing transition probabilities. The Lyman lines show an opposite behavior of increasing ordinate values with increasing upper level for $u \geq 8$, approaching the values for the Balmer lines. Only the centrally depressed Lyman lines with $u \leq 7$ show a slight decrease in the numbers of effectively emitting atoms for increasing u.

For an interpretation of the different behavior of Balmer and Lyman lines, we follow the NLTE calculations by Gouttebroze et al. (1993). The analysis of the Balmer lines by Stellmacher (1969) shows that the populations of the upper levels $u > 4$ follow, relative to each other, a smooth distribution with an equilibrium temperature of $T \approx 6000$ K. This value is close to the kinetic temperature $T_{kin} (\approx T_e)$ obtained from the line widths and is conform to the departure coefficients $b_u = 1$ for $u > 4$ calculated by Gouttebroze et al. (1993).

For the Lyman lines, these authors obtain a total optical prominence thickness equivalent to $\tau(\mathrm{Ly}_{22\to1}) = 230$ with "conventional" electron temperature $T_e = 8000$ K. For higher temperatures $T = 10\,000$ K and $T = 15\,000$ K (more realistic for a prominence corona transition atmosphere), their models still lead to values of $\tau(\mathrm{Ly}_{22\to1}) = 48$ and 2.5, respectively, even 1000 and 52 for $\mathrm{Ly}_{8\to1}$.

Emission lines with such high τ values will be limited to the outermost (hotter) prominence regions. A rough estimate shows that the geometric extention of the effectively emitting layers (which produce the emerging Lyman emission) is rather small as compared to that of the (optically thin) Balmer lines, which amounts to the whole prominence atmosphere.

In general, the geometric thickness H of an emitting layer can be estimated from

$$\tau_{u,1} = \frac{\sqrt{\pi} \cdot e^2}{m_e \cdot c^2} \cdot \frac{\lambda}{\Delta\lambda} \cdot \lambda \cdot f \cdot n_1 \cdot H. \qquad (3)$$

With $n_1 \approx 0.5 \cdot n_e = 2 \times 10^{10}$ cm^{-3} and $\Delta\lambda/\lambda = 1.2 \times 10^{-4}$ (as observed), one obtains a geometric thickness of only $H = 30$ km for $\mathrm{Ly}_{8\to1}$ assuming a high value of $\tau(\mathrm{Ly}_{8\to1}) = 20$.

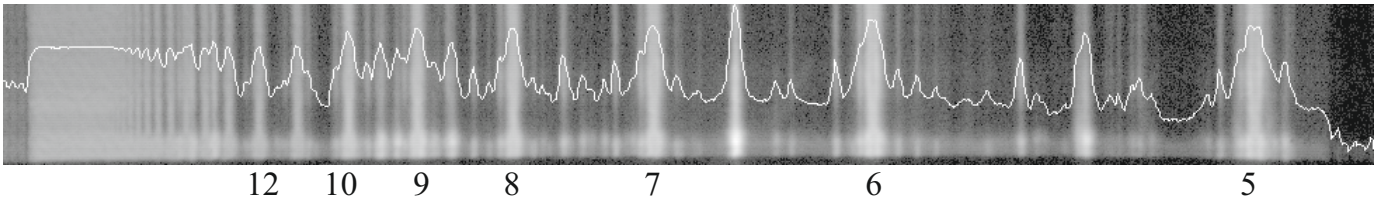

Fig. 2. SUMER spectrum of the prominence observed on July 8, 2000 by Stellmacher et al. (2003), showing the wavelength range 910 Å $< \lambda <$ 947 Å with the Lyman emissions ($u \geq 5$) along the 120″ slit, which covers 20″ of the upper chromosphere (lower image border), 30″ below the prominence, and 70″ of the prominence body. The white line gives the spectral radiance distribution averaged over the prominence body in a logarithmic scale. The jump between $u = 10$ and $u = 11$ is due to the different detector coating (KBr for larger λ). Note the largely constant spectral radiance of the Lyman line centers.

With increasing level number u, the total thickness decreases toward that of the Lyman continuum, for which Parenti et al. (2005b) still deduce $\tau(\mathrm{Ly}_{912}) \approx 6.5$, and the emissions will originate more and more in deeper (cooler) layers, thus approaching the main regions of Balmer line emissions. This readily explains both the 'bending' of the Lyman curves in Fig. 1 and their approach to the values of the optically thin ($u > 4$) Balmer lines. Upper levels $u \geq 12$ will largely be in equilibrium with the free electrons since their energy distance to the ionization limit amounts to only $\Delta E < 0.1$ eV.

3. Spectral radiance at the Lyman line centers

The spectral radiances at line center $L_{u1}(\lambda_0)$ are largely independent of u. This can be seen in the SUMER spectrum (Fig. 2) showing the Lyman emissions ($u \geq 5$) in the wavelength range 910 Å $< \lambda <$ 947 Å along the 120″ slit, which covers 20″ of the upper chromosphere (lower image border), 30″ below the prominence, and 70″ of the prominence body. Superposed is the mean spectral radiance distribution $L_{u1}(\lambda)$ over the prominence body in a logarithmic scale.

The almost constant central line radiances $L_{u1}(\lambda_0)$ indicate largely equal brightness temperatures T_b, which may be derived via the Planck function. For the optically thick Lyman lines ($\tau(Ly) \gg 1$, hence emitted from the prominence periphery), the spectral radiance at line center $L_{u1}(\lambda_0)$ becomes equal to the source function S_{u1}, which we set equal to the Planck function $B_{u1}(T_\mathrm{b})$.

In Table 1 we give the deduced T_b, together with the observed spectral radiance at the Lyman line centers $L_{u1}(\lambda_0)$ and the total spectral line radiance $E_{ul} = \int L^{\lambda}_{ul}\,\mathrm{d}\lambda$ for the brightest (42-L) and the faintest (70-H) prominence regions marked in Fig. 1 as rhombs and squares. The mean values of, respectively, $T_\mathrm{b} = 4989$ K and $T_\mathrm{b} = 4822$ K (neglecting the centrally most reversed line $u = 5$) show a small internal scatter of only ±20 K. The radiometric accuracy of 15% for detector A in the corresponding λ regime (Schühle et al. 2000) introduces an uncertainty of $\Delta T_\mathrm{b} = 20$ K.

The T_b values deduced for the Lyman lines are more than 1000 K higher than the T_ex deduced from the Balmer lines, for which Stellmacher (1969) finds 3250 K $< T_\mathrm{ex} <$ 3840 K in similarly bright prominences. Even the maximum value $T_\mathrm{ex} = 3900$ K, occasionally found for the (optically thick) Hα line in the brightest prominences by Stellmacher & Wiehr (2005) is still ≈1000 K below the T_b found for the Lyman lines. This indicates that the peripheral prominence regions, which emit the Lyman lines, are significantly hotter than the prominence cores, which emit the Balmer lines.

Table 1. Upper level u, wavelength λ_0[Å], spectral line radiance $E^{\mathrm{obs}}_{\mathrm{ul}}$[mW/(m^2 s sr)], spectral radiance at line center $L_{u1}(\lambda_0)$[mW/(m^2 s sr Å)], and corresponding brightness temperature T_b [K] for Lyman lines of the two prominence regions given in Fig. 1 as rhombs and squares.

u	λ_0	brightest			faintest		
		E^{obs}_{u1}	$L_{u1}(\lambda_0)$	T_b	E^{obs}_{u1}	$L_{u1}(\lambda_0)$	T_b
5	949.8	69.1	0.057	4899	25.9	0.022	4752
6	937.8	36.8	0.077	4999	14.1	0.031	4855
7	930.8	23.3	0.056	4979	9.0	0.023	4841
8	926.2	18.0	0.051	4985	6.9	0.020	4840
9	923.2	15.7	0.045	4979	6.0	0.016	4820
10	921.0	12.1	0.039	4966	4.2	0.014	4809
11	919.4	12.4	0.040	4977	4.2	0.015	4827
12	918.1	13.3	0.042	4991	3.6	0.012	4799
13	917.2	10.2	0.037	4975	4.2	0.016	4864
14	916.4	11.9	0.045	5009	2.9	0.011	4794
16	915.3	11.0	0.037	4983	3.6	0.014	4835
17	914.9	10.4	0.037	4985	7.9	0.012	4814
18	914.6	10.3	0.034	4973	2.6	0.012	4815
19	914.3	13.1	0.033	4970	4.2	0.011	4803

3.1. Influence of filling

Since most prominences are formed by numerous tiny "threads" (e.g. Lin et al. 2005), the actual spectral radiances at line center can be expected to be higher than the observed ones. The coronal material inbetween will not emit Lyman lines. Realistic filling factors are still unknown. If we assume a filling of 50%, the actual spectral radiances would be two times, for 10% filling 10 times greater than those in Table 1. The influence of filling on the eventually deduced T_b values is, however, rather weak, because the brightest Lyman line at $\lambda = 937.8$ Å yields 110 K (400 K) higher T_b for a 50% (10%) filling.

Such a weak influence of filling also seems to be indicated in the various observations of different prominences. In particular, emissions deduced from two-dimensional imaging at much higher spatial resolution (Stellmacher & Wiehr 1999; Stellmacher & Wiehr 2000) largely follow the same relations as from spectra of much lower spatial resolution.

4. Line widths

High temperatures for the Lyman emitting regions are also indicated from the line widths. The value $\Delta\lambda/\lambda = 0.4 \times 10^{-4}$ observed for the unsaturated higher Balmer lines by Stellmacher (1969) and by Stellmacher & Wiehr (1994) correspond to $T^{\mathrm{max}}_{\mathrm{kin}} \approx 8700$ K, if purely thermally broadened, or to 7500 K for a mean non-thermal broadening of 4 km s^{-1}.

In contrast, the widths $\Delta\lambda/\lambda = 1.1 \times 10^{-4}$ measured by Parenti et al. (2005a) for the higher Lyman lines with $u > 16$, correspond to an upper limit (since optically thick) of $T_{\rm kin}^{\rm max} \approx 66\,000$ K in the case of a purely thermal broadening. For the hydrogen formation temperature of 16 000 K, a non-thermal broadening of 28.5 km s^{-1} is required, in accordance with Stellmacher et al. (2003; Figs. 16 and 17) and with Parenti & Vial (2007). The typical kinetic temperature of 7500 K, deduced from the Balmer lines for the cool prominence body, would lead to a high non-thermal broadening of 31 km s^{-1}.

Slightly broader Lyman lines with $\Delta\lambda/\lambda = 1.25 \times 10^{-4}$ were measured by Stellmacher et al. They discuss that the actual values may be smaller, since the intrinsic SUMER profile seems to be underestimated. The EUV spectrograph is particularly adapted to broad emission lines from the hot corona rather than to narrow lines from cool prominences. Regardless of that uncertainty, the broadening of the Lyman lines yields much higher temperatures $T_{\rm kin}$ than that of the Balmer lines, in accordance with the difference in the brightness temperatures $T_{\rm b}$.

5. Conclusions

The comparison of observed Lyman and Balmer emissions from faint through "medium bright" quiescent prominences, characterized by $E(\mathrm{H}\beta) < 2 \times 10^4$ erg/(cm^2 s sr), shows that the inner regions with $T_{\rm kin} \approx 7500$ K that emit the optically thin Balmer lines are not those with much higher $T_{\rm kin}$ that emit the Lyman lines. Even different members of the Lyman series will not originate in the same prominence volume. The very high τ values of the first Lyman members will limit their emerging emission to the outermost prominence periphery where excitation and ionization are highest.

With decreasing $\tau \approx \lambda \cdot f$, higher Lyman members will originate more and more in the deeper layers. A realistic modeling of the Lyman and the Balmer lines will have to consider strong gradients between the cool prominence body and its hot periphery for temperature and (or) non-thermal velocities besides the strong departures from LTE.

Heinzel et al. (2001) propose that the reversed profiles of the stronger Lyman lines will be related to the orientation of the line-of-sight (LOS) with respect to the magnetic field lines: emissions viewed across the field lines are expected to show strong reversals. The calculations by Loucif & Magnan (1982) can be useful for profile modeling. They treat the transfer problem of emerging reversed lines taking spatially correlated velocity fields into account and applying the method of addition of layers.

From our various observations, we do not find systematic differences between prominences viewed under different aspect angles, but instead we find the largely unique emission relations displayed in Fig. 1. Observations at higher spatial resolution including the magnetic field might help for adapting more refined models.

Acknowledgements. We thank Dr. F. Hessman and I. E. Dammasch and for helpful discussions; B. Bovelet kindly performed the graphics in Fig. 1.

References

De Boer, C. R., Stellmacher, G., & Wiehr, E. 1998, A&A, 334, 280
Gouttebroze, P., Heinzel P., & Vial J.-C. 1993, A&AS, 99, 513
Heinzel, P., Schmieder, B., Vial, J.-C., & Kotrc, P. 2001, A&A, 370, 281
Illing, R. M. E., Landman, D. A., & Mickey, D. L. 1975, Sol. Phys., 45, 339
Loucif, M. L., & Magnan, C. 1982, A&A, 112, 287
Lin, Y., Engvold, O., Rouppe van der Voort, L., Wijk, J. E., & Berger, T. E. 2005, Sol. Phys., 226, 239
Parenti, S., & Vial, J.-C. 2007 ApJ, 469, 1109
Parenti, S., Vial, J.-C., & Lemaire, P. 2005a, A&A, 443, 679
Parenti, S., Vial, J.-C., & Lemaire, P. 2005b, A&A, 443, 685
Schühle, U., Curdt, W., Hollandt, J., et al. 2000, Appl. Opt., 36, 6416
Stellmacher, G. 1969, A&A, 1, 62
Stellmacher, G., & Wiehr, E. 1994, A&A, 290, 655
Stellmacher, G., & Wiehr, E. 2005, A&A, 431, 1069
Stellmacher, G., Wiehr, E., & Dammasch, I. E. 2003, Sol. Phys., 217, 133
Unsöld, A. 1955, Physik der Sternatmosphären, 2.Aufl. (Berlin: Springer)
Wiese, W. L., Smith, M. W., Glennon, B. M. 1966, Atomic Transition Probabilities, Vol. I, H through Ne, Nat. Stand. Ref. Data Ser., Nat. Bur. Stand. (US) 4, U.S.-Gov. Washington DC: Printing Office
Yakovkin, N. A., & Zel'dina, M. Yu. 1975, Sol. Phys., 45, 319